IEEE Access
Multidisciplinary ⋮ Rapid Review ⋮ Open Access Journal

Received 18 December 2022, accepted 22 January 2023, date of publication 31 January 2023, date of current version 8 February 2023.

Digital Object Identifier 10.1109/ACCESS.2023.3241244

RESEARCH ARTICLE

Domestic Load Management With Coordinated Photovoltaics, Battery Storage and Electric Vehicle Operation

NAROTTAM DAS[1,2], (Senior Member, IEEE), AKRAMUL HAQUE[3], HASNEEN ZAMAN[1], SAYIDUL MORSALIN[4], (Member, IEEE), AND SYED ISLAM[5], (Life Fellow, IEEE)

[1]School of Engineering and Technology, Central Queensland University, Melbourne, VIC 3000, Australia
[2]Centre for Intelligent Systems, Central Queensland University, Brisbane, QLD 4000, Australia
[3]Department of Electrical and Electronic Engineering, Premier University, Chittagong 4367, Bangladesh
[4]School of Electrical Engineering and Telecommunications, The University of New South Wales, Sydney, NSW 2052, Australia
[5]School of Engineering, Information Technology and Physical Sciences, Federation University Australia, Ballarat, VIC 3352, Australia

Corresponding authors: Narottam Das (n.das@cqu.edu.au) and Akramul Haque (akramul073@gmail.com)

This work was supported in part by the New Staff Research Grant, School of Engineering and Technology, Central Queensland University, Brisbane, QLD, Australia, in 2019, under Grant RSH5171; in part by the School of Engineering and Technology, Central Queensland University, Melbourne Campus, Melbourne, VIC, Australia; and in part by the Centre for Intelligent Systems, Central Queensland University.

ABSTRACT Coordinated power demand management at residential or domestic levels allows energy participants to efficiently manage load profiles, increase energy efficiency and reduce operational cost. In this paper, a hierarchical coordination framework to optimally manage domestic load using photovoltaic (PV) units, battery-energy-storage-systems (BESs) and electric vehicles (EVs) is presented. The bidirectional power flow of EV with vehicle to grid (V2G) operation manages real-time domestic load profile and takes appropriate coordinated action using its controller when necessary. The proposed system has been applied to a real power distribution network and tested with real load patterns and load dynamics. This also includes various test scenarios and prosumer's preferences e.g., with or without EVs, number of EV owners, number of households, and prosumer's daily activities. This is a combined hybrid system for hierarchical coordination that consists of PV units, BES systems and EVs. The system performance was analyzed with different commercial EV types with charging/ discharging constraints and the result shows that the domestic load demand on the distribution grid during the peak period has been reduced significantly. In the end, this proposed system's performance was compared with the prediction-based test techniques and the financial benefits were estimated.

INDEX TERMS Autoregressive integrated moving average (ARIMA), coordinated operation, cost reduction, domestic load management, electric vehicle (EV), energy management, moving average (MA).

NOMENCLATURE

$\psi^{EV}_{\max}$	Maximum state of charge level.
$\psi^{EV}_{\min}$	Minimum state of charge level.
λ^{EV}_{th}	EV's SOC threshold limit.
$\Theta^{EV}_{t,\chi}$	Charging or discharging state/mode of an EV.
$\eta_1, \eta_2, \eta_3, \eta_4$	Efficiency of converters 1, 2, 3 and 4 respectively.
$p^{EV}_{t,\chi}$	The net power gained by EV.
Φ_χ	represents the battery capacity of an EV.
$\overline{\Re}^p_t$	Base load demand.
$\Re^p_t$	Domestic power demand.
m	peak-load occurrence frequency.
n	off-peak load occurrence frequency.
$P^{BES_+}_{tot}$	maximum power available from the BESs.

The associate editor coordinating the review of this manuscript and approving it for publication was Chandan Kumar.

$P_{tot}^{PV_+}$	maximum power available from PV units.
τ_p	Peak load.
τ_b	Base load.
$\hat{C}_E^{BES}$	Cost of the energy supplied by the battery storage system.
μ_{DoD}	Depth of discharge.

I. INTRODUCTION

Traditionally, power grids are centrally managed and supply electricity to consumers through a network of long-distance transmission and distribution lines. Conventional power systems nowadays see a significant paradigm shift towards an automated and distributed trend of energy management. The huge influx of small-scale and aggregated renewable energy resources (e.g., solar, wind) at the domestic or distribution level creates multiple power management challenges to the utilities [1], [2], [3]. This is because most of these renewable sources are intermittent in nature, and so maintaining the power quality according to standard voltage and frequency requirements is a significant challenge [2], [3].

As a new type of dynamic load, electric vehicles (EVs) are also now being integrated into the power networks. Unlike standalone battery energy storage (BES) systems, the mobility of EVs makes their in-built energy storage capability more dynamic than the fixed installation storages [4], [5], [6]. The bidirectional power flow from an EV, in residential areas or aggregated EVs in a parking lot through grid-to-vehicle (G2V) and vehicle-to-grid (V2G) operation, has the potential to provide ancillary support and various loads to the power grids [6], [7], [8]. Moreover, the adverse effects due to the intermittent behavior of renewables and vehicle's uncertainty related to their availability can be lessened with the combination of EVs and fixed energy storages [2], [4]. To reduce the energy usage cost, these energy storages perform charging operations during off-peak periods (i.e., the duration of low energy cost), while during peak-load periods (i.e., the duration of high electricity demand and price), their discharging operation potentially assists in reducing the peak-load at domestic sides [4], [8]. Any load profile is likely to have multiple increasing peaks over time; therefore, if these peak loads are not coordinately or regularly managed on domestic sides, these will cause adverse effects to nearby power network components (e.g., distribution transformer, power cables, and protection circuitry) [4], [5], [6], [7].

In this context, a coordinated or regulated power demand management is essential to minimize the peak-load effects and maximize the utilization of distributed resources [9], [10], [11]. Additionally, it reduces the energy costs for customers during peak-load periods and incentivizes customers when there is less demand [8], [11]. With coordinated management, sometimes various forecasting techniques are implemented for the purpose of scheduling as well as optimizing the energy resources [2], [12]. Thus, it has the potential benefits of improving power quality (i.e., increasing PV voltage and reducing flicker voltage), stability management (i.e., voltage and frequency) and power regulation (balancing power flow) [9], [10], [12]. For domestic load management, till now, the majority of previous work is either considered rooftop PV units with different household battery sizes or mere integration of EVs. Domestic BESs used in a small-scaled microgrid provide various ancillary support considering managing load, frequency or voltage [4], [13]. The peak-load management with EVs in commercial systems is elaborately reported in [11]. The impacts of integrating large-scale battery-storage system for managing increasing demand are also examined in [9] and [13]. In [14], using a decision-tree-based algorithm, a combination of PV, EV, and different battery systems are used at domestic levels to manage the peak load; however, the contribution from each energy source at any time interval and economic aspects are found to be inadequate. The particle swarm optimisation-based energy management system has been applied among the smart home, EVs and PV farm without the consideration of BESs [15]. While, the reduction of peak load using scheduling has been done in [16], without discussing the economic benefit. A hybrid approach for energy demand forecast using autoregressive integrated moving average model has been studied and reported in [17], [18], [19], and [20].

Moreover, the majority of previously developed systems were applied only for a short duration; but the effectiveness of these systems in reducing the peak load considering the real test case scenario for a longer duration is still unclear [8], [21]. For example, in [22], authors developed a load curve manually and scheduled the load with respect to energy rates and PV generations but did not consider any real scenario. Therefore, it has a huge interest to examine the effectiveness of a hybrid system consisting of an EV, PV, and battery storage on real test environments over longer periods. In other words, each resource's contribution at the domestic level with respect to time intervals and load dynamics is a subject yet to be explored. In this paper, a coordinated system consisting of PV units, BES systems and EVs is considered for managing the domestic peak load demand. A hierarchical coordination framework is developed and tested on a real environment of distribution networks in Australia. Three types of commercial EVs with small (Mitsubishi-i-MiEV), medium (Nissan Leaf) and large (Tesla-3) battery sizes are considered for load management. An improved scheduling algorithm is also developed for their charging and discharging operation, while the intended future extension of this project will include the performance comparison of various optimization algorithms applications in the proposed microgrid. For analyzing the economic aspects, real-time load pricing from the Australian energy market is used to study the financial benefits of the proposed management framework. To sum up, the main contributions of this paper are as follows:

- Develop an improved domestic energy management framework to manage the domestic load profile and utilize resources in a more efficient and economical way.

- Identify a coordinated approach considering each dynamic source constraint and load contribution for managing distributed resources and peak demand.
- Investigate the peak load reduction process under real test scenarios of uncertainties and seasonal conditions by considering dynamic and environment-dependent sources and load profiles for a longer duration.
- The acceptance of the proposed system is verified with various test case conditions, such as EV types, source combinations, number of EV owners, number of households, prosumer's daily activities etc.
- Compare the performance of the developed system with moving average (MA) and autoregressive integrated moving average (ARIMA) prediction systems.
- Study the financial aspects of the designed framework.

II. SYSTEM OVERVIEW

The schematic diagram of a small-scaled microgrid is shown in Fig. 1. The microgrid model comprises residential households (or loads) and energy sources (a PV panel, battery storage, and an electric vehicle). Depending on the prosumer and the number of households, EVs and BES's number will be more than one. All energy sources are connected to a common AC bus through power electronic converters. Both the BES and EV have bidirectional power flow capabilities. A central controller is attached to the residential places which regularly monitors the load pattern, PV power generation, load demand, BES, EV's state of charge (SOC), and charging-discharging condition. Depending on load requirements, conditions, and resources (i.e., PV, battery and EV) availability, the controller will make the charging or discharging operation of both BES and EV either from the PV or from the AC bus, respectively.

A. ELECTRIC VEHICLE SPECIFICATIONS

There are three commercial V2G capable electric vehicles with different battery sizes (i.e., small, medium, and large) considered for load management. These are Mitsubishi-i-MiEV, Nissan Leaf and Tesla Model 3. Each car belongs to a single household. The total energy consumed or served by the EV depends on the user profile of the EV owner [23], [24]. To comply with the prosumer's habit in real life, three different charging profiles (for people going to work during the daytime, people staying at home, and people working on night shifts) are considered. For the daytime working profile, the vehicle owner leaves home at 9.00 am and returns at 4.00 pm. There are no charging facilities available at the workplace parking area. To avoid any undesirable situation, the EV battery will never fall below the minimum state of charge (SOC) level. Here, all assumptions are taken into account for simulation, and analysis purposes only and these can be modified based on a more available realistic scenario. For example: in [25], the authors build a hybrid (power grid and communication) model and considered the EV's status during the transit period also, which brings a more realistic view of the practical scenario. In this work, for simplicity, the instantaneous SOC of the EVs during the transit period has not been considered. However, all key parameters related to the EV specifications are given in Table 1. The station, process and bay level are connected to each other by two buses- the process bus and station bus [26].

B. BES AND PV's SPECIFICATION

Each house has its own PV panel and BES system. For simulation purposes, it is assumed that the energy generation from each house (i.e., either PV panel or BES) is similar. The detailed specifications of the PV panel and BES are listed in Table 2.

III. MATHEMATICAL MODEL FOR ENERGY MANAGEMENT

Overall energy management of the whole microgrid system is performed following an optimization algorithm implemented in a central controller. The detailed architecture of the whole microgrid system is shown in Fig. 2. The central controller is connected to various smart meters and converters (Conv-1, 2, 3, 4). Conv-4 (dc-dc) and Conv-2 (dc-ac) connect the PV panel to the AC bus, while Conv-3 (dc-dc) connects the BES with PV via a DC bus when there is a surplus PV generation during daytime. On the other hand, both the battery and EV are connected to the AC bus via bidirectional power flow functionality type (i.e., DC-AC and AC-DC) converters.

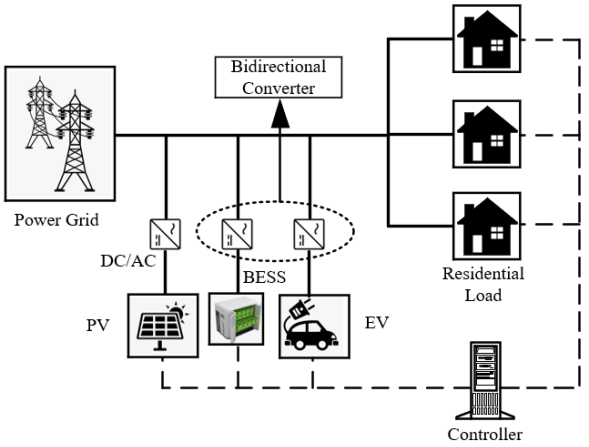

FIGURE 1. Overview of a small-scaled microgrid.

TABLE 1. EV specifications used in the simulation.

Electric Vehicle	Mitsubishi -i-MiEV	Nissan Leaf	Tesla Model 3
Maximum battery capacity (kWh)	16	40	50
Maximum power (kW)	3.3	6.6	7.7
Maximum number of EVs	3		
Efficiency of EV charger	90% [19]		
EV's SOC threshold limit (Δ_{th}^{EV})	90% [18], [19]		
EV's minimum SOC level ($\psi_{\min}^{EV}$)	25% [18]		

TABLE 2. PV specifications used in the simulation.

Parameter	Specifications
PV panel in each house and average capacity	1, 3.3 kW
PV degradation	2% per annum
Efficiency of the converter used for PV and battery.	95%
Maximum BES capacity	10-24 kWh
BES lifecycle	> 10 k
Efficiency of BES (charging/discharging)	90%

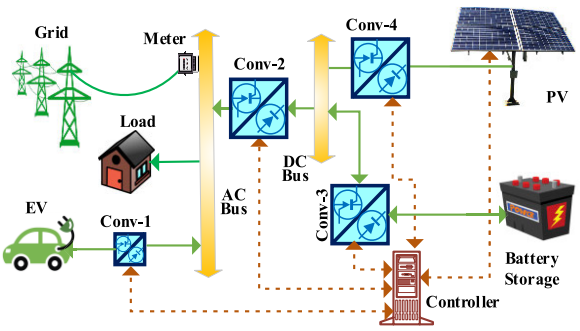

FIGURE 2. Detailed architecture of developed management framework.

The power flow (i.e., inward or outward current) of these converters entirely depends on the residential load conditions and local energy generation. On the other hand, the controller regularly reads the domestic load demand, power generation, availability of resources and the real-time electricity cost from the utility to check the peak load managed energy price steps. The implemented optimization technique follows a set of mathematical programming problems considering technical or system constraints of PV units, BESs, and EVs integrated into the grid. The overall aim is to reduce total systems costs and ensure efficient use of energy resources. The step-by-step mathematical models for each network component are described in the following sub-sections.

A. EV WITH ENERGY TRANSACTION

An EV participates in energy transactions through the charging or discharging process of its in-built battery storage. The charged or discharged amount is limited by two boundary points: (a) minimum state of charge level (ψ_{min}^{EV}) and (b) maximum state of charge level ψ_{max}^{EV}. Depending on load conditions, the EV will go only to V2G operation if it exceeds the certain threshold limit (ψ_{max}^{EV}) usually set by the manufacturers. Moreover, between the minimum SOC level ψ_{min}^{EV} and maximum charging limit ψ_{max}^{EV}, the charging power relates to the state of charge level by a linear piecewise function and can be expressed as of (1), as shown at the bottom of the page, [8], [14]:

In this paper, any contribution to the grid (i.e., power injected into the grid) is shown with +'ve superscript, while any power taken from the grid is labelled with 've superscript. Here, for the V2G operation, the maximum available power from an EV during the discharging process can be expressed as follows:

$$\Gamma_t^{EV+} \cong \left(\Gamma_{\max}^{EV} - \Gamma_{th}^{EV}\right) * \left(1 - \frac{\psi_t^{EV} - \lambda_{th}^{EV}}{\psi_{\max}^{EV}}\right); \quad \lambda_{th}^{EV} < \psi_t^{EV} \leq \psi_{\max}^{EV} \tag{2}$$

Let us assume, be a set of periods for which an EV of a micro-grid system is plugged for either G2V or V2G operation, where, X means the total number of EVs of the concerned area. The limiting constraints of charging or discharging power can be written as follows:

$$0 \leq \Gamma_{t,\chi}^{EV-} \leq \Gamma_{\max}^{EV} \Theta_{t,\chi}^{EV}; \forall t \in \xi_\chi, \forall \chi \in X \tag{3}$$

$$0 \leq \Gamma_{t,\chi}^{EV+} \leq \Gamma_{\max}^{EV} (1 - \Theta_{t,\chi}^{EV}); \forall t \in \xi_\chi, \forall \chi \in X \tag{4}$$

$$\Gamma_{t,\chi}^{EV+} \leq \Gamma_{t,\chi}^{EV-}; \forall t \in \xi_\chi, \forall \chi \in X \tag{5}$$

Here, the binary variable $\Theta_{t,\chi}^{EV}$ represents the charging or discharging state/mode of an EV. The value $\Theta_{t,\chi}^{EV}$ varies for the following conditions:

$$\Theta_{t,\chi}^{EV} = \begin{cases} 1; & \text{If EV is in charging mode} \\ 0; & \text{If EV is in discharging mode} \end{cases} \tag{6}$$

On the other hand,$\Gamma_{t,\chi}^{EV-} \geq 0$, $\Gamma_{t,\chi}^{EV+} \geq 0$ denote the charged power to the battery and the discharged power from the battery to the grid respectively.

When an EV completes the journey for the purpose of work and returns home, the energy required by the vehicle is ℓ_χ^{EV+} for the period of $\forall t \in T \backslash \xi_\chi$. Then, the net energy $p_{t,\chi}^{EV}$ at any time interval $\Delta\tau$ can be written as follows:

$$p_{t,\chi}^{EV} \cong \begin{cases} \left(\eta_1 \, \Gamma_{t,\chi}^{EV-} - \Gamma_{t,\chi}^{EV+} / \eta_1\right) \Delta\tau; & \forall t \in \xi_\chi, \forall \chi \in X \\ -\ell_\chi^{EV+}; & \forall t \in T \backslash \xi_\chi, \forall \chi \in X \end{cases} \tag{7}$$

Here, $\boldsymbol{\eta_1}$ denotes the efficiency of converter 1. The net power gained $p_{t,\chi}^{EV}$ by an EV in relation to the SoC level at

$$\Gamma_t^{EV-} \cong \begin{cases} \left(\Gamma_{th}^{EV} / \lambda_{th}^{EV}\right) \psi_t^{EV}; & \psi_{min}^{EV} < \psi_t^{EV} < \lambda_{th}^{EV} \\ \left(\Gamma_{max}^{EV} - \Gamma_{th}^{EV}\right) + \left(\Gamma_{th}^{EV} / \lambda_{th}^{EV}\right) \psi_t^{EV}; & \lambda_{th}^{EV} < \psi_t^{EV} < \psi_{max}^{EV} \\ \Gamma_{th}^{EV}; & \psi_t^{EV} \leq \psi_{min}^{EV} \end{cases} \tag{1}$$

an interval $\boldsymbol{\Delta\tau}$ can be calculated from the following set of equations.

$$p_{t,\chi}^{EV_{net}} = \Phi_\chi\ \psi_{t,\chi}^{EV} - \Phi_\chi\ \psi_{t-1,\chi}^{EV}; \forall t \in T, \forall \chi \in X \tag{8}$$

$$\psi_{t,\chi}^{EV} - \psi_{t-1,\chi}^{EV} = \psi_{I,\chi}^{EV}; t \geq 1, \forall \chi \in X \tag{9}$$

Here, Φ_χ represents the battery capacity of an EV and $\psi_{I,\chi}^{EV}$ denotes the instantaneous SOC of EV. Note that each house will maintain a maximum of one vehicle in a plugged-in state at each period $t \in T$. Therefore, the number of EVs plugged into a microgrid system will be equal to or lower than the number of households κ. This can be expressed by following constraints.

$$\prod_{t,\chi}^{plug} = \sum_{\chi=1}^{X} \Theta_{t,\chi}^{EV} + \sum_{\chi=1}^{X} (1 - \Theta_{t,\chi}^{EV}) \leq \kappa; \forall t \in \xi_\chi, \forall \chi \in X \tag{10}$$

and

$$\prod_{t,\chi}^{plug} \equiv \begin{cases} \geq 1; & \forall t \in \xi_\chi, \forall \chi \in X \\ 0; & \forall t \in T \backslash \xi_\chi, \forall \chi \in X \end{cases} \tag{11}$$

For $\prod_{t,\chi}^{plug} \geq 1$, the microgrid must be either receiving or feeding energy to the EVs; however, any plugged-in EV will not participate in both energy transactions at the same time [27]. Therefore, the total electric power P_{tot}^{EV} derived from all EVs ($\forall \chi \in X$) in a microgrid system at any test period ($\forall t \in \xi_\chi$) can be written as:

$$\left[P_{tot}^{EV} = \prod_{t,\chi}^{plug} \sum_{\chi=1}^{X} \left(\Gamma_{t,\chi}^{EV-} + \Gamma_{t,\chi}^{EV+} \right) \right] \leq \prod_{t,\chi}^{plug} \Gamma_{\max}^{EV} \tag{12}$$

The domestic load curve is always a function of power (p) and time (t). Note that the total domestic load demand at the common AC bus must be equal to or greater than the total consumers' power demand connected to that bus. Since the phase voltage at that common bus does not vary significantly with the load change, so only the load current varies depending on the consumers' power demand.

B. MICROGRID POWER DEMAND

In a microgrid system, the domestic power demand $\Re_t^p$ and the consumers' desired base load demand $\overline{\Re}_t^p$ are always a function of independent variables time (t) and power (p), and are expressed as below [28]:

$$\Re_t^p = \phi(p, t) \tag{13}$$

$$\overline{\Re}_t^p = \phi(p_\lambda, t) \tag{14}$$

Domestic BES and EVs always read base load (off-peak) and peak-load periods for their charging and discharging operation. The load periods (peak/ off-peak), in sub-second timescale, are usually sensed by the controller. These may occur several times within a finite duration regardless of whether it is a day or month. Let's assume the peak load starts at τ_s^p and ends at τ_e^p, while the off-peak load initiates at τ_s^b and stops at τ_e^b.

If the peak load and off-peak load occurrence frequency are designated as m and n, respectively, then the total time period T can be expressed as the summation of both peak-load (τ_p) and base load (τ_b) periods and is given by

$$T = m \left(\sum_{\tau_s^p}^{\tau_e^p} \tau_p \right) + n \left(\sum_{\tau_s^b}^{\tau_e^b} \tau_b \right) \tag{15}$$

The difference between the domestic power demand ($\Re_t^p$) and consumers' baseload demand ($\overline{\Re}_t^p$) determines the off-peak and peak-load periods. The required power ($P_t^{req} \in \Re_t^p$) demand, whether peak or off-peak, at t^{th} instant ($t \in \tau_p, \tau_b$) can be written as follows:

$$P_t^{req} = \Re_t^p - \overline{\Re}_t^p \tag{16}$$

The peak load and baseload periods are determined by the following equation,

$$P_t^{req} \equiv \begin{cases} \geq 0; & \text{peak-load demand condition} \\ < 0; & \text{off-peak demand condition} \end{cases} \tag{17}$$

C. PEAK-LOAD CONDITION

For $P_t^{req} \geq 0$ at t^{th} instant, the power difference is supplied by the available energy resources to balance the load demand. In this case, the energy sources (i.e., PVs, BESs, EVs) will provide the required power to the common AC bus. Let P_{tot}^{BES+} and P_{tot}^{PV+} be the maximum power available from the BESs and PV units, respectively. Hence, the power balance equation of any microgrid system can be written as follows:

$$P_t^{req} = P_{tot}^{PV+} + P_{tot}^{EV} + P_{tot}^{BES+} = \sum \left\langle P_{tot}^{PV+}, P_{tot}^{EV}, P_{tot}^{BES+} \right\rangle \tag{18}$$

If $P_{tot}^{EV} = 0$; the EVs are not in a plugged-in state and not available to act as either a source or sink, the mismatched power $\left\{ P_t^{req} - \sum \left\langle P_{tot}^{PV+}, P_{tot}^{EV}, P_{tot}^{BES+} \right\rangle \right\}$ is supplied from the AC bus. Assume the lower SOC boundary and the instantaneous SOC for a BES are ψ_{min}^{BES} and ψ_t^{BES}, respectively. Therefore, the maximum power received from a battery unit installed in a household $\psi_t^{BES} \geq \psi_{min}^{BES}$ is given by the following equations:

$$p_t^{BES+} = \eta_2 * \eta_3 * \Phi_{BES} \left(\psi_t^{BES} - \psi_{\min}^{BES} \right); \forall p_t^{BES+} \in P_{tot}^{BES+} \tag{19}$$

$$P_{tot}^{BES+} = \kappa * p_t^{BES+} \tag{20}$$

$$P_{tot}^{PV+} = \eta_4 * \kappa * P_\kappa^{PV+} \tag{21}$$

Here, Φ_{BES} is the capacity of the battery storage unit. η_2 and η_3 denote the efficiencies of converter 2 and converter 3 respectively, P_κ^{PV+} is the average PV power generation per household and η_4 denotes the efficiency of converter 4.

D. OFF-PEAK CONDITION

For off-peak periods ($P_t^{req} < 0$), the available grid power P_t^{grid} can be used to charge the energy storages (i.e., EVs and BESs), so under this condition, the power-balance equation can be written as follows:

$$\overbrace{\overline{\Re}_t^p - \Re_t^p}^{off-peak} + P_{tot}^{PV+} = P_{tot}^{BES-} + P_{tot}^{EV} \tag{22}$$

$$P_t^{grid} = \overline{\Re}_t^p - \Re_t^p \tag{23}$$

$$P_{tot}^{BES-} = \kappa * p_t^{BES-} \tag{24}$$

In this case, the amount of power required to charge a BES varies according to the difference between the maximum charging limit and SoC status. So, the maximum charging power requested by a BES (p_t^{BES-}) is given by (25)

$$p_t^{BES-} = \eta_2 * \eta_3 * \Phi_{BES} \left(\psi_{\max}^{BES} - \psi_t^{BES} \right); \quad \forall p_t^{BES-} \in P_{tot}^{BES-} \tag{25}$$

Here, $\psi_{\max}^{BES}$ represents a maximum charging limit of battery storage. On the other hand, EVs will charge up to the requested power according to (1).

E. POWER SOURCES, LOADS AND POLARITY

During the peak load and off-peak load periods, depending on the charging and discharging process, the number of energy sources and loads vary in order to balance the power-demand equation. At any time instant ($t \in \tau_p \cup \tau_b \in T$), the total supply sources (P_{tot}^S) and loads (P_{tot}^L) connected to the main AC bus can be written as follows [28].

For $P_t^{req} < 0$(off-peak),

$$P_{tot}^L \approx \begin{cases} \underbrace{\Re_t^p}_{Household\ load} \\ \underbrace{\kappa * \eta_2 * \eta_3 * \Phi_{BES} \left(\psi_t^{BES} - \psi_{\min}^{BES} \right)}_{Battery\ Storages} \\ \underbrace{\prod_{t,\chi}^{plug} \sum_{\chi=1}^{X} \left(\Gamma_{t,\chi}^{EV-} + \Gamma_{t,\chi}^{EV+} \right)}_{EVs} \end{cases} \tag{26}$$

and for $P_t^{req} \geq 0$(peak-load), is defined by equation (27).

The polarity of power flow from any energy source indicates whether it will act as a source or sink. In other words, any positive polarity in the simulation results represents the action as a source; conversely, negative polarity indicates the load operation. Moreover, the power flow polarity identifies the charging and discharging mode of an EV and battery.

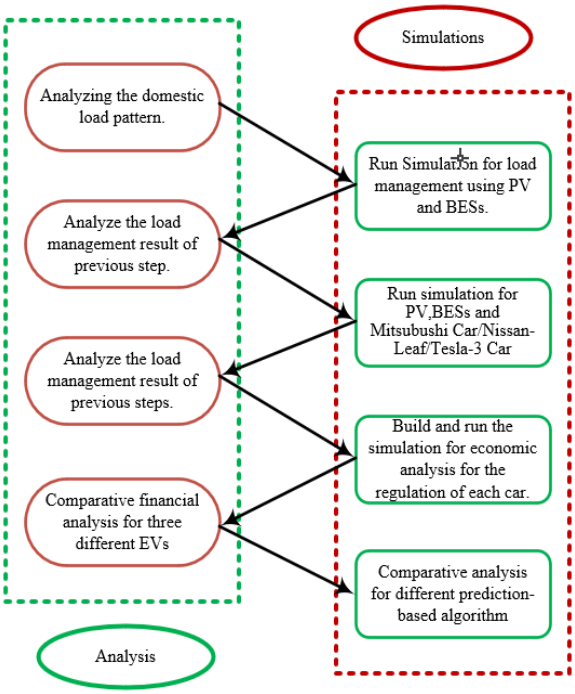

FIGURE 3. Working methodology of the proposed research work.

$$P_{tot}^S \approx \begin{cases} \underbrace{\eta_4 * \kappa * P_{\kappa}^{PV+}}_{PVs} \\ \underbrace{\kappa * \eta_2 * \eta_3 * \Phi_{BES} \left(\psi_{\max}^{BES} - \psi_t^{BES} \right)}_{Battery\ Storages} \\ \underbrace{\prod_{t,\chi}^{plug} \sum_{\chi=1}^{X} \left(\Gamma_{t,\chi}^{EV-} + \Gamma_{t,\chi}^{EV+} \right)}_{EVs} \\ \underbrace{\overline{\Re}_t^p - \Re_t^p}_{Grid} \end{cases} \tag{27}$$

F. ALGORITHM OF POWER DEMAND MANAGEMENT

The algorithm proposed to manage the domestic load is shown in Table 3 followed by two flowcharts as in Fig. 10 and Fig. 11. It includes the coordinated operation of EV, BES and PV for shaving the power demand of a real-time load curve.

IV. CASE STUDIES ON A REAL NETWORK

The total working methodology of this paper has been depicted in Fig.3. While, Fig. 4 shows the proposed control framework which has been applied to a real power distribution network located in the Nelson Bay area of New South Wales (NSW), Australia. All relevant information on network configuration, load pattern, demand response and available resources were obtained from a trial 'Smart Grid, Smart City (SGSC) project funded by the Australian Government in collaboration with Energy Australia, Ausgrid, and other

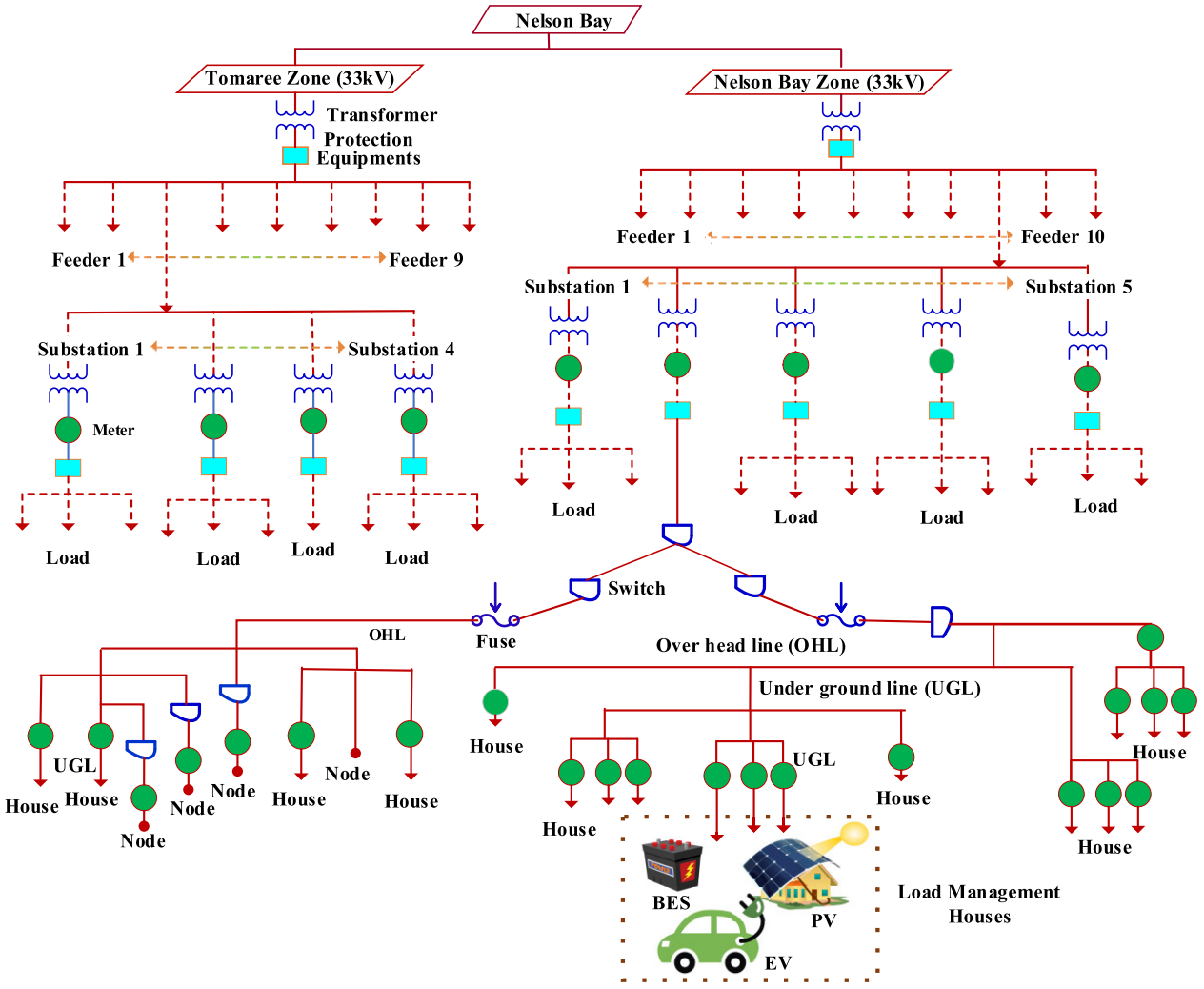

FIGURE 4. Real Australian distribution network located in Nelson Bay and Tomaree zone, NSW.

consortium partners like Nelson Bay City Council, Sydney Water, GE Energy Australia etc. [26], [29]. The majority of loads in this area are more likely residential, rural and small industries and are serviced by two 33-kV substations located in Tomaree and Nelson Bay, NSW.

The efficacy of the proposed system and control framework for managing the domestic loads was tested on three neighbouring households (H1, H2 and H3). These customers are powered through a long feeder from Nelson Bay substation and experience seasonal load changes. Climate data were also used here to evaluate the average PV unit's generation and weather dependent load pattern. The average load curves of H1, H2 and H3 in three consecutive days are illustrated in Fig. 5 and the corresponding analysis with several test case scenarios is described in the following subsections.

The average PV generation at each house is 3.3 kW and each house has placed 40-kWh battery storage. In this paper, the available baseload (or average) demand is considered as 9 kW from 12.00 pm-11.59 pm and 6.8 kW from 12.00 am-11.59 am. Therefore, the peak load condition is more likely

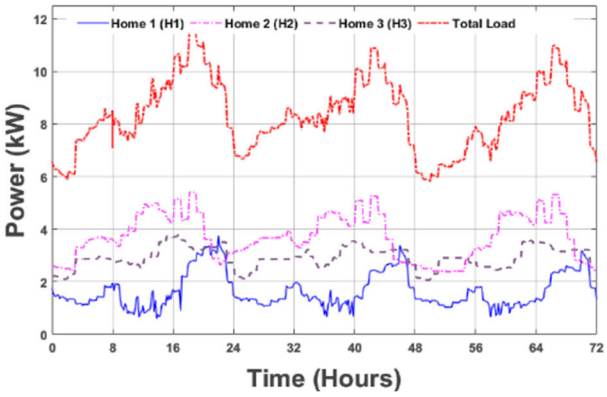

FIGURE 5. Load patterns of residential households at nelson bay area.

to be observed from 7 am to 9 am in the first half (because of lower PV generation) and from 6 pm to 10 pm in the second half of any test period day (because of higher domestic load demand). These assumptions are realistic, completely

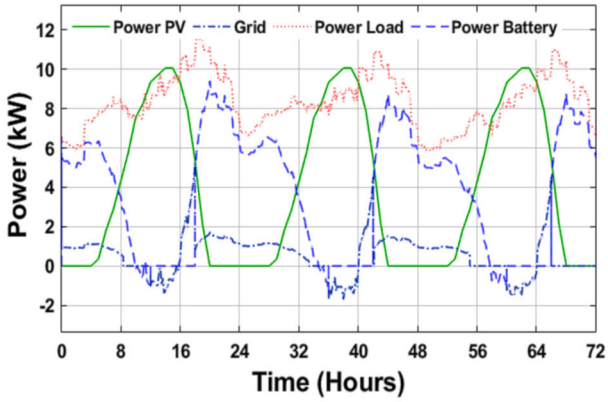

FIGURE 6. Load management with PV and 40 kwh BESs.

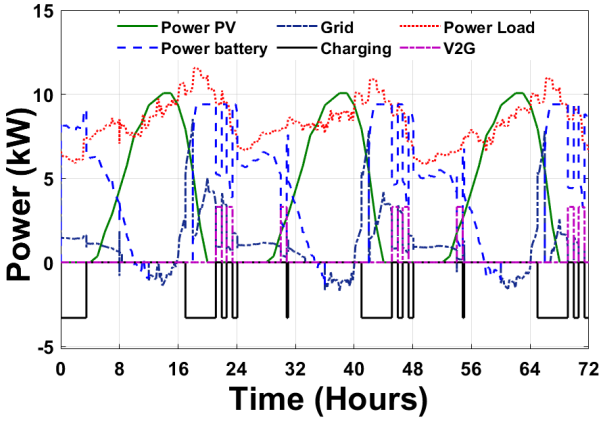

FIGURE 7. Management with PV, BESs and Mitsubishi EV.

complying with the actual load demand pattern given by the Australian Energy Market Operator (AEMO) [30]. Initially, the PV power is not available, and the battery storage is charged up to the maximum level. To enhance the battery lifetime by reducing the depth of discharge (DoD), the BES charging/ discharging limit is maintained within 40 $\sim$ 95% of the SOC level [31]. In this research, 60% of DoD has been considered.

A. LOAD MANAGEMENT WITH PV AND BES

The load demand management of three households with controlled PV and battery storage operation is shown in Fig. 6. The PV power generation is based on the irradiation curve found in [32]. As can be observed, with the controlled operation, during the off-peak period the households receive a large proportion of active power from either battery storage (especially, at night-time) or PV units (especially, during daytime). If any surplus energy generation happens, the microgrid system returns additional power to the grid or charges the BES. In Fig. 6, this can be identified as the negative polarity of the grid and battery power. On the other hand, the consumption of grid power reaches a maximum during the peak period because the battery storage is solely not capable to supply any additional power requirement to balance the load demand. It happens two times per day, first in the morning and second happens after the evening when PV power is absent.

B. LOAD MANAGEMENT WITH PV, BESs AND EV TYPES

In this case study, the combined response for managing domestic loads using the PVs, battery storages and a commercial EV from three different types: Mitsubishi, Nissan Leaf and Tesla-3 is discussed. As described earlier, these commercial EVs have their own in-built small, medium and larger battery and their coordinated response are shown in Fig. 7, Fig. 8 and Fig. 9 respectively. From Fig. 7, it is evident that during the peak period after battery storage operation, if any additional power is required, the controlled system, instead of taking power from the grid, mitigates the required energy demand with the V2G operation of the Mitsubishi. Unlike Nissan Leaf and Tesla-3 vehicles, due to smaller battery sizes, the Mitsubishi performs more charging and discharging within 24 hours. It is because it can reach its highest and lowest SOC limit faster than the other two types of cars. In fact, for its lower charge capacity, it needs a charging operation after each V2G operation. On the other hand, during the off-peak period occurs, if the EV is in the plugged-in state, then it will be likely to be charged from available resources. For EVs, here the constant voltage constant current charging topology has been considered; hence the charging power is constant.

In Fig. 7, Fig. 8 and Fig. 9, during 10.00 am - 5.00 pm, PV generation is maximum, so in this period, after managing the domestic load and charging the BESs, the excess PV energy is directly transferred to the AC bus through the converters 2 and 4. If an EV is available at home after coming from work (4.00-7.00 pm) and the PV and BES power are not sufficient to charge the EV and manage the load demand, then the shortfall is drawn from the common AC bus.

As expected, and observed in Fig. 9, due to the larger battery size, the Tesla-3 model manages more load demand and thereby, provides comparatively a higher load factor during the peak period than that of other EV types. The effectiveness of the proposed system is also tested with the load conditions of two households and found similar results of managing the load demand regardless of conditions whether it is peak or off -peak period.

C. THREE HOUSEHOLDS HAVING EVs

Instead of having a single EV, the proposed system is considered with three EVs, where each house has just one EV type and the combined response is shown in Fig. 12. It is found that the developed system is independent to load pattern and network component's constraints. However, the power consumption from the AC bus, in this case, is found to be higher and less V2G duration is observed due to the higher aggregated battery power consumed by all EVs. The charging curves are not constant for the whole charging period, because, in the graph, the combined charging power is shown. Where

TABLE 3. The real-time domestic load management algorithm in pseudo-code.

	Tasks
1:	**Determine:** time instant $t \in \tau_p \cup \tau_b \in T$
2:	**Evaluate:** power demand $\Re_t^p = \phi(p,t)$ and baseload $\overline{\Re}_t^p = \phi(p_\lambda,t)$
3:	**Calculate:** $P_t^{req} = \Re_t^p - \overline{\Re}_t^p$
4:	**while** $P_t^{req} \geq 0$ $\left(\Re_t^p \geq \overline{\Re}_t^p\right)$
5	{**Calculate:** the required load support from available sources P_{tot}^S
6	**Check:** Total PV power generation P_{tot}^{PV+}
7	**if** $P_{tot}^{PV+} \geq P_t^{req}$
8	..... $P_{tot}^{PV+} \rightarrow P_t^{req}$
9	**elseif** $P_{tot}^{PV+} < P_t^{req}$
10	**Check:** boundary conditions of BES: ψ_t^{BES} and $\psi_{\min}^{BES}$ **Calculate:** P_{tot}^{BES+}
11	**if** $\left\{P_t^{req} - \Sigma\left\langle P_{tot}^{PV+}, P_{tot}^{BES+}\right\rangle\right\} \geq 0$
12	**Check:** EV's availability $\prod_{t,\chi}^{plug} \geq 1$, boundary constraint $\psi_{\max}^{EV}$, Δ_t^{EV} and Δ_{th}^{EV} ; calculate P_{tot}^{EV}
13	$P_t^{req} \rightarrow \Sigma\left\langle P_{tot}^{PV+}, P_{tot}^{EV}, P_{tot}^{BES+}\right\rangle$
14	**else**
15	$P_t^{req} \rightarrow \Sigma\left\langle P_{tot}^{PV+}, P_{tot}^{BES+}\right\rangle$ }
16	Iteration continues and check condition in 4
17	**while** $P_t^{req} < 0$ $\left(\Re_t^p < \overline{\Re}_t^p\right)$
18:	{**Calculate:** supply power demand to available loads P_{tot}^L
19	**Check:** Total PV power generation $P_{tot}^{PV+} \geq 0$
20	**Check:** boundary conditions of BES: ψ_t^{BES} and $\psi_{\max}^{BES}$;calculate P_{tot}^{BES-}
21	**Check:** EV's availability $\prod_{t,\chi}^{plug} \geq 1$, boundary constraint $\psi_{\min}^{EV}$, Δ_t^{EV} and $\psi_{\max}^{EV}$; calculate P_{tot}^{EV}
22	**If** $P_{tot}^{PV+} \geq P_{tot}^L$
23	$P_{tot}^{PV+} \rightarrow P_{tot}^L$
24	**elseif** $P_{tot}^{PV+} < P_{tot}^L$
25	**Calculate:** P_t^{grid} and $P_t^{grid} \geq 0$
26	$\Sigma\left\langle P_{tot}^{PV+}, P_t^{grid}\right\rangle \rightarrow P_{tot}^L$ }
27	Iteration continues and check conditions in 4 and 17

Tesla-3 is charging for the longest period for its highest battery capacity.

V. COST-BENEFIT ANALYSIS

This section aims to demonstrate the cost-benefit analysis of the domestic load management system. Let's assume the unit cost of the energy supplied by the battery storage system is

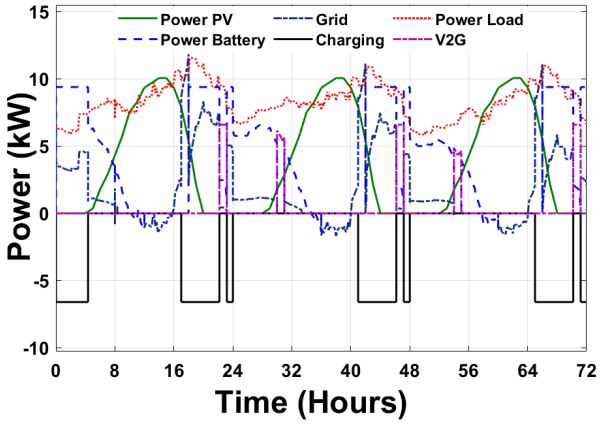

FIGURE 8. Management with PV, BESs and Nissan Leaf EV.

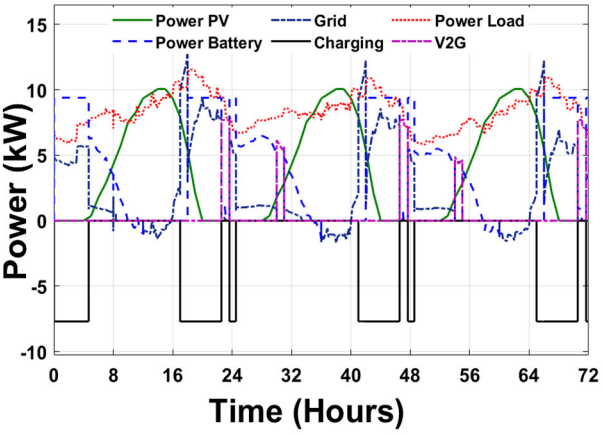

FIGURE 9. Load management with PV, BES and Tesla-3 EV.

$\hat{C}_E^{BES}\hat{C}_E^{BES}$. It is calculated by dividing the total installation and maintenance cost of the BESs by the total energy generated from BESs (W_A^{BES}), and can be written as follows [11]:

$$\hat{C}_E^{BES} = (C_I^{BES} + C_{OMC}^{BES}) \Big/ W_A^{BES} \tag{28}$$

where, W_A^{BES} can be found by multiplying the instantaneous discharged power, the number of the charge-discharge cycle with the discharging time length and the operating duration in a year (in days). Mathematically, the W_A^{BES} can be written as:

$$W_A^{BES} = p_t^{BES} \times \sum\nolimits_{i=1}^{n} (D_i \times L_i) \times \eta \times H_0 \tag{29}$$

The per-year battery cost ($\hat{C}_B$) can be formulated by adding together the per unit battery cell ($C_{b,pu}$) cost, the battery management cost ($C_{m,pu}$) and the cost of power equilibrium (C_{eq}). It can be expressed as follows.

$$\hat{C}_B = C_{b,pu} + C_{m,pu} + C_{eq} \tag{30}$$

The total battery converter cost P_C^{BES} can be calculated by multiplying the per unit battery converter cost with the BES capacity. If the installation, maintenance, and operation cost

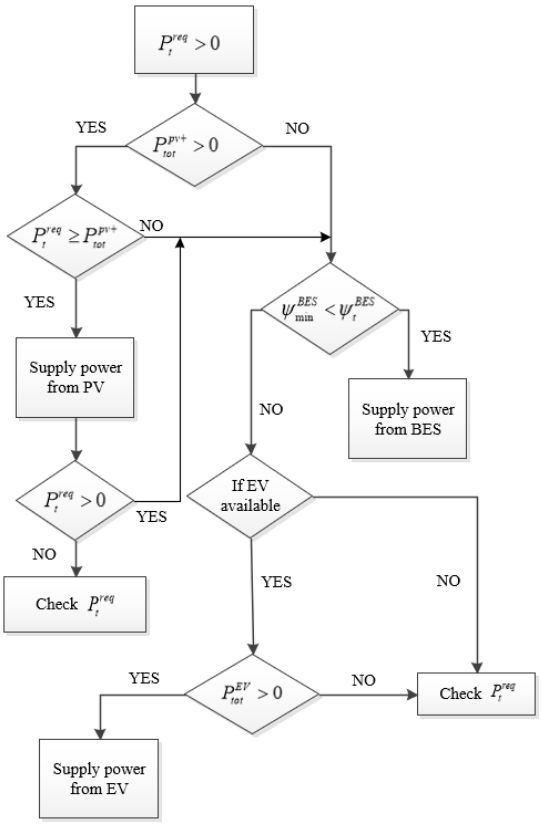

FIGURE 10. Flowchart for domestic load during peak time.

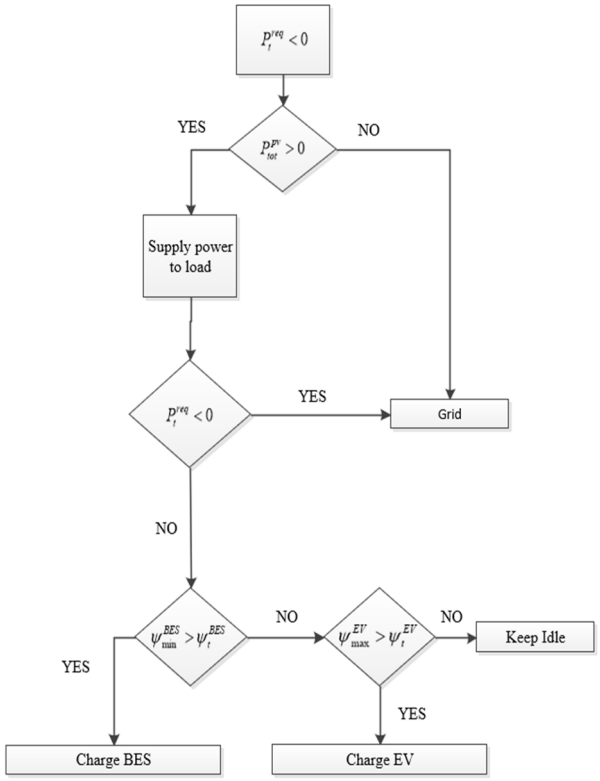

FIGURE 11. Flowchart for domestic load during off-peak-time.

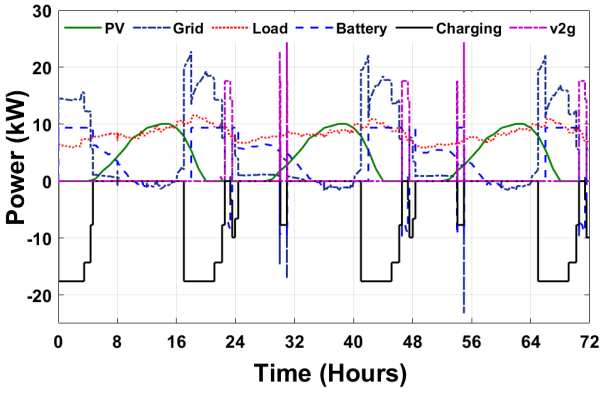

FIGURE 12. Load management with Mitsubishi, Nissan Leaf and Tesla-3.

for each kWh of battery storage is $\hat{C}_{f,B}$, the total installation, maintenance, and operation cost $C_{f,B}$ can be calculated by the following (31),

$$C_{f,B} = \hat{C}_{f,b} \times P_C^{BES} \tag{31}$$

It is also needed to calculate the salvage value of the storage battery and deduct it from the energy cost of the BESs. If the initial and lost capacity of the battery are Q_i and Q_{loss} respectively, then the salvage value of the BESs S_C is

$$S_C = Q_i - Q_{loss} \tag{32}$$

It should be noted that the battery capacity can be lost due to cycle or calendar fading or ageing. Battery ageing is governed by various charging/discharging and chemical factors and therefore, an accurate prediction of the battery ageing model is quite difficult. A semi-empirical approach is proposed in [33], where the Q_{loss} has been related to the discharging current rate (I_d), and charge output (A_H) as follows:

$$Q_{loss} = \beta \ \exp\left\{\left(-3.17 \times 10^4 + 370.3 \times I_d\right)\Big/ GT\right\} \times A_H^{0.55} \tag{33}$$

Here, β is a pre-exponent factor which is inversely related with I_d. The complete charging/discharging impact (or degradation) on the battery life L_d by considering the temperature impacts μ_T and depth of discharge (DoD) μ_{DoD} is given as:

$$L_d = \mu_{DoD} \times \mu_T \times L_{rat} \tag{34}$$

Here, L_{rat} is the rated battery life cycle. Based on the AEMO electricity price during peak and off-peak periods in 2020 [30], the cost-benefit analysis of the proposed system with any of the Mitshubishi, Nissan Leaf and Tesla EVs is illustrated in Fig. 13. It can be observed that the coordinated operation of EV shows much better performance in terms of energy cost than that of the unregulated management. Note that the electricity price data here are based on the summer season of NSW in Australia and fed directly into the controller to calculate the total energy cost. It is shown

that, the energy price has been reduced to 38.18% due to the regulated use of Mitshubishi in the summer season, which is 6.5% more than the article [15]. The benefit will grow more for the longer use of the proposed energy management system.

VI. COMPARISON WITH OTHER MODELS

With the controlled operation of PV, BESs and a Nissan Leaf EV, the proposed system is compared with different prediction-based controlled techniques, such as moving average (MA) and autoregressive integrated moving average system (ARIMA). Autoregressive model predicts depending on the previous error, so it does not change instantaneously. Moving average (MA) is a better process as it depends on the past value of prediction and had been used for years for load forecasting [34]. Autoregressive MA (ARMA) model predicts data using both error and predicted past value. The autoregressive integrated MA (ARIMA) is a more advanced tool compared to ARMA. The ARIMA Model is especially appealing since it uses logical and well-organized processes to create models utilizing the autocorrelation and partial autocorrelation functions [35]. During load forecasting, the relatively weak response of the ARIMA model to sudden disturbances makes it more preferable to implement [36]. In this research, a simple model MA and an advanced model ARIMA have been considered. The comparison is depicted in Fig. 14 and it confirms that the proposed control strategy shows similarly improved performance in reducing the peak load demand with other prediction techniques.

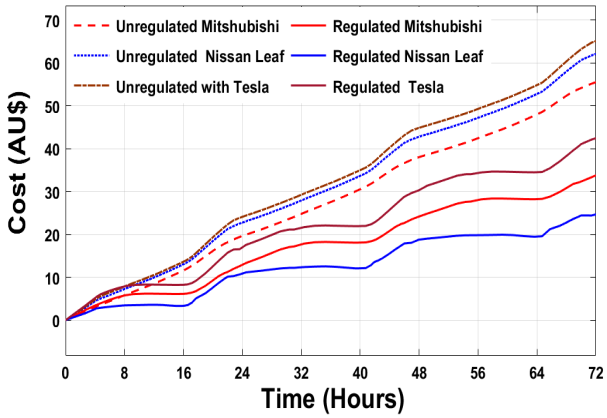

FIGURE 13. Cost-benefit analysis with the proposed system.

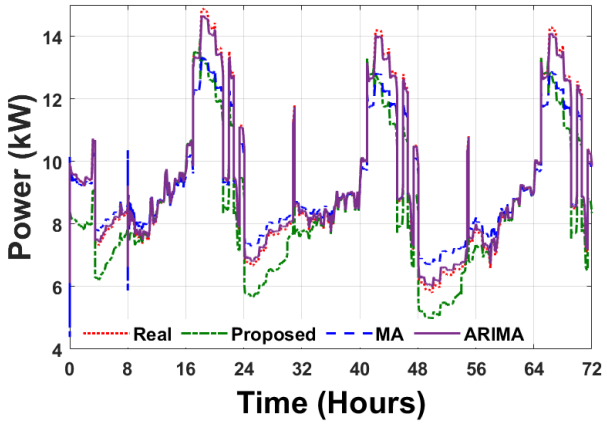

FIGURE 14. Comparison of the proposed system with different prediction techniques.

VII. CONCLUSION

This paper presents an improved framework of managing domestic load demand with the coordinated operation of photovoltaics (PVs), battery energy storages (BESs) and electric vehicles (EVs). Three commercial EVs with small (Mitshubishi i-MiEV), medium (Nissan Leaf) and large (Tesla) battery sizes with respect to the domestic load pattern in a real power distribution network were used to examine and validate the designed network performance. These studies showed that, under realistic circumstances, the developed framework can significantly reduce the peak load demand on the AC main grid. Moreover, an EV with the larger battery capacity can manage more peak domestic loads comparing to other EV types, thus suggesting an improved utilization of electricity infrastructure.

The findings were further supported by the cost-benefit analysis using the real energy price given by a local energy distributor. Under these realistic load patterns, the developed framework was also compared with prediction-based techniques and similar improved performances in managing domestic energy demand were found. These results will be useful for both efficient and economic utilization of distributed energy resources and their coordinated management.

REFERENCES

[1] M. Liserre, T. Sauter, and J. Y. Hung, "Future energy systems: Integrating renewable energy sources into the smart power grid through industrial electronics," *IEEE Ind. Electron. Mag.*, vol. 4, no. 1, pp. 18–37, Mar. 2010, doi: 10.1109/MIE.2010.935861.

[2] C. F. Calvillo, A. Sánchez-Miralles, and J. Villar, "Synergies of electric urban transport systems and distributed energy resources in smart cities," *IEEE Trans. Intell. Transp. Syst.*, vol. 19, no. 8, pp. 2445–2453, Aug. 2018.

[3] M. H. Rehmani, M. Reisslein, A. Rachedi, M. Erol-Kantarci, and M. Radenkovic, "Integrating renewable energy resources into the smart grid: Recent developments in information and communication technologies," *IEEE Trans. Ind. Informat.*, vol. 14, no. 7, pp. 2814–2825, Jul. 2018, doi: 10.1109/TII.2018.2819169.

[4] S. A. El-Batawy and W. G. Morsi, "Optimal design of community battery energy storage systems with prosumers owning electric vehicles," *IEEE Trans. Ind. Informat.*, vol. 14, no. 5, pp. 1920–1931, May 2018, doi: 10.1109/TII.2017.2752464.

[5] S. Morsalin, K. Mahmud, and G. E. Town, "Scalability of vehicular M2M communications in a 4G cellular network," *IEEE Trans. Intell. Transp. Syst.*, vol. 19, no. 10, pp. 3113–3120, Oct. 2018, doi: 10.1109/TITS.2017.2761854.

[6] A. A. Munshi and Y. A.-R. I. Mohamed, "Extracting and defining flexibility of residential electrical vehicle charging loads," *IEEE Trans. Ind. Informat.*, vol. 14, no. 2, pp. 448–461, Feb. 2018, doi: 10.1109/TII.2017.2724559.

[7] K. Knezovic, S. Martinenas, P. B. Andersen, A. Zecchino, and M. Marinelli, "Enhancing the role of electric vehicles in the power grid: Field validation of multiple ancillary services," *IEEE Trans. Transport. Electrific.*, vol. 3, no. 1, pp. 201–209, Oct. 2017, doi: 10.1109/TTE.2016.2616864.

[8] L. Igualada, C. Corchero, M. Cruz-Zambrano, and F.-J. Heredia, "Optimal energy management for a residential microgrid including a vehicle-to-grid system," *IEEE Trans. Smart Grid*, vol. 5, no. 4, pp. 2163–2172, Jul. 2014, doi: 10.1109/TSG.2014.2318836.
[9] S. Bashash and H. K. Fathy, "Cost-optimal charging of plug-in hybrid electric vehicles under time-varying electricity price signals," *IEEE Trans. Intell. Transp. Syst.*, vol. 15, no. 5, pp. 1958–1968, Oct. 2014.
[10] F. Sehar, M. Pipattanasomporn, and S. Rahman, "An energy management model to study energy and peak power savings from PV and storage in demand responsive buildings," *Appl. Energy*, vol. 173, pp. 406–417, Jul. 2016, doi: 10.1016/J.APENERGY.2016.04.039.
[11] K. Mahmud, M. J. Hossain, and J. Ravishankar, "Peak-load management in commercial systems with electric vehicles," *IEEE Syst. J.*, vol. 13, no. 2, pp. 1872–1882, Jun. 2019, doi: 10.1109/JSYST.2018.2850887.
[12] G. Li, C. C. Liu, C. Mattson, and J. Lawarree, "Day-ahead electricity price forecasting in a grid environment," *IEEE Trans. Power Syst.*, vol. 22, no. 1, pp. 266–274, Feb. 2007, doi: 10.1109/TPWRS.2006.887893.
[13] M. Rowe, T. Yunusov, S. Haben, C. Singleton, W. Holderbaum, and B. Potter, "A peak reduction scheduling algorithm for storage devices on the low voltage network," *IEEE Trans. Smart Grid*, vol. 5, no. 4, pp. 2115–2124, Jul. 2014, doi: 10.1109/TSG.2014.2323115.
[14] K. Mahmud, M. J. Hossain, and G. E. Town, "Peak-load reduction by coordinated response of photovoltaics, battery storage, and electric vehicles," *IEEE Access*, vol. 6, pp. 29353–29365, 2018, doi: 10.1109/ACCESS.2018.2837144.
[15] M. Ben Arab, M. Rekik, and L. Krichen, "Suitable various-goal energy management system for smart home based on photovoltaic generator and electric vehicles," *J. Building Eng.*, vol. 52, Jul. 2022, Art. no. 104430, doi: 10.1016/J.JOBE.2022.104430.
[16] D. Kucevic, S. Englberger, A. Sharma, A. Trivedi, B. Tepe, B. Schachler, H. Hesse, D. Srinivasan, and A. Jossen, "Reducing grid peak load through the coordinated control of battery energy storage systems located at electric vehicle charging parks," *Appl. Energy*, vol. 295, Aug. 2021, Art. no. 116936, doi: 10.1016/J.APENERGY.2021.116936.
[17] F. Kaytez, "A hybrid approach based on autoregressive integrated moving average and least-square support vector machine for long-term forecasting of net electricity consumption," *Energy*, vol. 197, Apr. 2020, Art. no. 117200.
[18] M. Akil, E. Dokur, and R. Bayindir, "Energy management for EV charging based on solar energy in an industrial microgrid," in *Proc. 9th Int. Conf. Renew. Energy Res. Appl. (ICRERA)*, Sep. 2020, pp. 489–493.
[19] E. D. Kostopoulos, G. C. Spyropoulos, and J. K. Kaldellis, "Real-world study for the optimal charging of electric vehicles," *Energy Rep.*, vol. 6, pp. 418–426, Nov. 2020.
[20] A. Zahedmanesh, K. M. Muttaqi, and D. Sutanto, "A consecutive energy management approach for a VPP comprising commercial loads and electric vehicle parking lots integrated with solar PV units and energy storage systems," in *Proc. 1st Global Power, Energy Commun. Conf. (GPECOM)*, Jun. 2019, pp. 242–247.
[21] V. Gupta, S. R. Konda, R. Kumar, and B. K. Panigrahi, "Multiaggregator collaborative electric vehicle charge scheduling under variable energy purchase and EV cancelation events," *IEEE Trans. Ind. Informat.*, vol. 14, no. 7, pp. 2894–2902, Jul. 2018, doi: 10.1109/TII.2017.2778762.
[22] A. Mohammad, M. Zuhaib, I. Ashraf, M. Alsultan, S. Ahmad, A. Sarwar, and M. Abdollahian, "Integration of electric vehicles and energy storage system in home energy management system with home to grid capability," *Energies*, vol. 14, no. 24, p. 8557, Dec. 2021.
[23] P. B. Andersen, T. Sousa, A. Thingvad, L. S. Berthou, and M. Kulahci, "Added value of individual flexibility profiles of electric vehicle users for ancillary services," in *Proc. IEEE Int. Conf. Commun., Control, Comput. Technol. Smart Grids (SmartGridComm)*, Oct. 2018, pp. 1–6, doi: 10.1109/SMARTGRIDCOMM.2018.8587585.
[24] J. Zhang, J. Yan, Y. Liu, H. Zhang, and G. Lv, "Daily electric vehicle charging load profiles considering demographics of vehicle users," *Appl. Energy*, vol. 274, Sep. 2020, Art. no. 115063.
[25] B. Sah, P. Kumar, R. Rayudu, S. K. Bose, and K. P. Inala, "Impact of sampling in the operation of vehicle to grid and its mitigation," *IEEE Trans. Ind. Informat.*, vol. 15, no. 7, pp. 3923–3933, Jul. 2019, doi: 10.1109/TII.2018.2886633.
[26] B. C. G. Lewis, A. Murray, M. Weight, and B. Anderson, "Customer applications, SGSC technical compendium," in *Proc. Smart Grid Smart City (SGSC)*, Sydney, NSW, Australia, 2014, pp. 1–234.
[27] S. Morsalin, K. Mahmud, and G. Town, "Electric vehicle charge scheduling using an artificial neural network," in *Proc. IEEE Innov. Smart Grid Technol.-Asia (ISGT-Asia)*, Nov. 2016, pp. 276–280, doi: 10.1109/ISGT-ASIA.2016.7796398.
[28] K. Mahmud, M. S. Rahman, J. Ravishankar, M. J. Hossain, and J. M. Guerrero, "Real-time load and ancillary support for a remote island power system using electric boats," *IEEE Trans. Ind. Informat.*, vol. 16, no. 3, pp. 1516–1528, Mar. 2020, doi: 10.1109/TII.2019.2926511.
[29] K. Proctor, "GA1675—Smart grid PS+EDGE modelling platform," in *Proc. Smart Grid Smart City*, Sydney, NSW, Australia, 2014, pp. 9–59.
[30] *Quarterly Energy Dynamics Q1 2020*, AEMO, Melbourne, VIC, Australia, 2020.
[31] L. Setyawan, J. Xiao, and P. Wang, "Optimal depth-of-discharge range and capacity settings for battery energy storage in microgrid operation," in *Proc. Asian Conf. Energy, Power Transp. Electrific. (ACEPT)*, 2017, pp. 1–7.
[32] X. Liu and Z. Bie, "Cooperative planning of distributed renewable energy assisted 5G base station with battery swapping system," *IEEE Access*, vol. 9, pp. 119353–119366, 2021, doi: 10.1109/ACCESS.2021.3108041.
[33] J. Wang, P. Liu, J. Hicks-Garner, E. Sherman, S. Soukiazian, M. Verbrugge, H. Tataria, J. Musser, and P. Finamore, "Cycle-life model for graphite-$LiFePO_4$ cells," *J. Power Sources*, vol. 196, no. 8, pp. 3942–3948, Apr. 2011, doi: 10.1016/J.JPOWSOUR.2010.11.134.
[34] S. A. A. Karim and S. A. Alwi, "Electricity load forecasting in UTP using moving averages and exponential smoothing techniques," *Appl. Math. Sci.*, vol. 7, pp. 4003–4014, Jan. 2013.
[35] S. Gn, "Short-term load forecasting using ARIMA model for Karnataka state electrical load," *Int. J. Eng. Res. Develop.*, vol. 13, pp. 75–79, Oct. 2017.
[36] E. Chodakowska, J. Nazarko, and Ł. Nazarko, "ARIMA models in electrical load forecasting and their robustness to noise," *Energies*, vol. 14, no. 23, p. 7952, Nov. 2021.

NAROTTAM DAS (Senior Member, IEEE) received the B.Sc. degree (Hons.) in electrical and electronic engineering from the Chittagong University of Engineering and Technology, Chittagong, Bangladesh, the M.Sc. degree in electrical and electronic engineering from the Bangladesh University of Engineering and Technology, Dhaka, Bangladesh, and the Ph.D. degree in electrical engineering from Yamagata University, Japan. He is currently a Senior Lecturer of electrical engineering at the School of Engineering and Technology, Central Queensland University, Melbourne, VIC, Australia. He has about three decades of experience as an academia and an Industrial Engineer in Australia and overseas. His Ph.D. research project was funded by the Ministry of Education, Sports and Culture, Government of Japan. He is the author/coauthor of over 200 peer-reviewed journals and international conference proceedings, including eight book chapters and four edited books, such as *Nanostructured Solar Cells*, *Advances in Optical Communication*, *Optical Communications*, and *Optical Communication System*. His research interests include power systems communication (smartgrids) using IEC 61850, multi-junction solar (PV) cells, modeling of high efficiency solar cells (renewable energy), and high-speed communication devices. He is a Senior Member of the IEEE PES and PHS, USA; a fellow of the Institution of Engineers, Australia, CPEng, and NER; and a Life Fellow of the Institution of Engineers, Bangladesh. He is the Guest Editor of the MDPI journal *Energies*, Special Issue on Nano-Structured Solar Cells and the *Journal of Nanomaterials* (Hindawi), Special Issue on Nano-Structured Thin-Film Materials and Surfaces Engineering Applications.

AKRAMUL HAQUE received the B.Sc. degree (Hons.) in electrical and electronic engineering and the M.Sc. degree in engineering from the Chittagong University of Engineering and Technology (CUET), Bangladesh, in 2013 and 2021, respectively. He has been working as an Assistant Professor of electrical and electronic engineering at Premier University, Chittagong, Bangladesh, since 2020, where he worked as a Lecturer, from 2015 to 2019. Earlier, he worked as a Quality Assurance Engineer at a transformer manufacturing company named "Integral Electric Company," Chittagong. His research interests include distributed energy resources (photovoltaic, wind energy, and battery storages) integration to the microgrid, electric vehicle coordination, energy management, and power systems stability and control.

HASNEEN ZAMAN received the B.Sc. degree (Hons.) in electrical and electronic engineering from the Chittagong University of Engineering and Technology, Chittagong, Bangladesh, in 2013, and the Graduate Certificate in Research (GCR) with major in electrical engineering from Central Queensland University (CQUniversity), Australia, in 2021, where she is currently working as a Research Assistant. Before moving to Australia, she worked as a Lecturer of electrical and electronic engineering at East Delta University, Chittagong. She also worked as an Assistant Electrical Engineer at Surprise Industrial Corporation, Chittagong. She has completed her industrial training (Internship) at the Training Institute for Chemical Industries (TICI), Narsingdi, Dhaka, Bangladesh. Her research interests include smart grid communications for modern power system networks and digital signal processing. She is a member of the Institute of Engineers, Bangladesh (IEB).

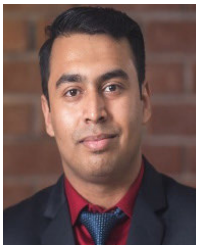

SAYIDUL MORSALIN (Member, IEEE) received the B.Sc. degree (Hons.) in electrical and electronic engineering from the Chittagong University of Engineering and Technology, Bangladesh, in 2013, the M.Res. degree (Hons.) from Macquarie University, Australia, in 2016, and the Doctor of Philosophy (Ph.D.) degree from the Energy Systems Research Group, The University of New South Wales (UNSW), Sydney, Australia, in 2020. His research interests include smart grid, diagnostic testing in high-voltage engineering, and power systems. He received the Dean's Award for his Ph.D. degree.

SYED ISLAM (Life Fellow, IEEE) received the B.Sc., M.Sc., and Ph.D. degrees in electrical power engineering, in 1979, 1983, and 1988, respectively. Currently, he is the Executive Dean and a Professor at the School of Science, Engineering and Information Technology, Federation University, Ballarat, Melbourne, VIC, Australia. He has been a keynote speaker and an invited speaker at many international workshops and conferences. His research interests include condition monitoring of transformers, wind energy conversion, and power systems. He has published over 300 technical papers in his area of expertise. He is a member of the Steering Committee of the Australian Power Institute. He is also a fellow of the Engineers Australia, the IEEE IAS, the IEEE PES, the IEEE DEIS, and the IET. He received the IEEE T. Burke Haye's Faculty Recognition Award, in 2000. He is the Current Chair of the Australasian Committee for Power Engineering (ACPE). He is a regular Reviewer of the IEEE TRANSACTIONS ON ENERGY CONVERSION, IEEE TRANSACTIONS ON POWER SYSTEMS, and IEEE TRANSACTIONS ON POWER DELIVERY. He was an Editor of the IEEE TRANSACTION ON SUSTAINABLE ENERGY. He is a Chartered Engineer at U.K. He is also an IEEE PES Distinguished Lecturer.